Low Complexity Erasure Insertion in RS-Coded SFH Spread-Spectrum Communications With Partial-Band Interference and Nakagami-m Fading

Lie-Liang Yang, *Member, IEEE,* and Lajos Hanzo, *Senior Member, IEEE*

***Abstract*—In this paper we propose two novel low-complexity, low-delay erasure insertion schemes, namely, the output threshold test (OTT) and joint maximum output and ratio threshold Test (MO-RTT). The employment of the OTT and MO-RTT is beneficial in the context of the "errors-and-erasures" Reed–Solomon (RS) decoding in a slow frequency-hopping spread-spectrum (SFH/SS) system using M-ary frequency-shift keying (MFSK). The statistics of the erasure insertion related decision variables associated with the OTT, MO-RTT as well as with the ratio threshold test (RTT) are investigated, when the channel of each frequency-hopping (FH) slot is modeled as flat Nakagami-m fading. The transmitted signals also experience both additive white Gaussian noise (AWGN) as well as partial-band Gaussian interference (PBGI). The properties of these erasure insertion schemes are investigated with the aid of their statistics. The performance of the proposed erasure insertion schemes and that of the erasure insertion scheme using the RTT is investigated and compared in the context of RS coded SFH/SS systems using MFSK. Furthermore, the performance of the RS coded SFH/SS systems is also compared both with and without side-information concerning the PBGI.**

***Index Terms*—Errors-and-erasures decoding, frequency-hopping, joint maximum output and ratio threshold test, M-ary frequency-shift keying, Nakagami fading, output threshold test, partial band interference, ratio threshold test, Reed–Solomon codes, spread-spectrum communications.**

I. Introduction

In SLOW frequency-hopping (SFH) spread-spectrum (SFH/SS) communication systems forward error-correction (FEC) using, for example Reed–Solomon (RS) codes is often used, in order to mitigate the performance degradation due to background noise, intentional and unintentional interference as well as channel fading [1]–[4]. In the context of the RS coded SFH/SS systems using M-ary frequency-shift keying (MFSK) data modulation [1], [2], "errors-and-erasures" decoding is preferable to "error-correction-only" decoding, since "errors-and-erasures" decoding can typically achieve a significantly lower codeword decoding error probability, than "error-correction-only" decoding, provided that a reliable erasure insertion scheme is invoked. By definition, the codeword decoding error probability is the probability of the event that a transmitted codeword cannot be successfully recovered by the decoder. In recent years the performance of RS coded SFH/SS systems using "errors-and-erasures" decoding based on erasure insertion schemes, such as the ratio threshold test (RTT) [4]–[13] or the Bayesian approach [14]–[18], has received wide attention. In the RTT [5] the ratio of the maximum to the "second maximum" of the decision variables, which are input to the maximum likelihood decision (MLD) unit of the M-ary orthogonal demodulator is observed, in order to make a decision whether an erasure is inserted or a RS code symbol is output by the demodulator. By contrast, in the context of the Bayesian approach [4] all the decision variables input to the MLD unit are observed for making an erasure decision.

In this contribution two novel erasure insertion schemes, namely the output threshold test (OTT) and the joint maximum output and ratio threshold test (MO-RTT) are proposed. The OTT uses only the maximum of decision variables input to the MLD unit, i.e., the actual output of the M-ary orthogonal demodulator, in order to make an erasure decision. By contrast, in the MO-RTT both the M-ary orthogonal demodulator's output involved in the OTT and the ratio involved in the RTT [5] are observed, in order to make an erasure decision. The above erasure insertion schemes have a similar complexity to that of the classic RTT [5], when employed in RS coded SFH/SS systems using MFSK. In this paper, the performance of the OTT, RTT and MO-RTT is investigated, when the channel is modeled as a flat Nakagami-m fading channel [20] and the transmitted signals are also subjected to partial-band gaussian interference (PBGI) [3]. We derive the exact Probability Density Functions (PDF) of the decision variables for making erasure insertion decisions associated with the OTT, RTT and the MO-RTT erasure insertion schemes over flat Nakagami-m fading channels, under the hypotheses that the M-ary demodulated symbol is correct (H_1) and incorrect (H_0). These PDFs are then used to investigate the characteristics of the OTT, RTT as well as MO-RTT over the above-mentioned Nakagami-m fading channels. With the aid of these PDFs, the expressions of symbol erasure probability and random symbol error probability after erasure insertion are derived, in order to evaluate the codeword decoding error probability of the RS coded SFH/SS systems invoking the OTT, RTT or MO-RTT. The performance of the RS coded SFH/SS system using MFSK data modulation assisted by "errors-and-erasures" decoding

Paper approved by C. Schlegel, the Editor for Coding Theory and Techniques of the IEEE Communications Society. Manuscript received January 4, 2001; revised July 20, 2001. This work was carried out in the framework of the IST Project IST-1999-12070 TRUST, which is partly funded by the European Union. This paper appeared in part at Globecom 2001, San Antonio, TX, November 25–29, 2001, pp. 796–800.

The authors are with the Department of Electronics and Computer Science, University of Southampton, Southampton SO17 1BJ, UK (e-mail: lly@ecs.soton.ac.uk; lh@ecs.soton.ac.uk).

Publisher Item Identifier S 0090-6778(02)05556-3.

employing the OTT, RTT and MO-RTT is then evaluated and compared with each other. Furthermore, the performance of the RS coded SFH/SS systems is investigated both with and without perfect side-information concerning the PBGI inflicted.

The remainder of this paper is organized as follows. In the next section, previous work concerning the SFH/SS system using MFSK modulation in the presence of PBGI is reviewed, and the required statistics of the M-ary decision variables are derived over the flat Nakagami-m fading channels considered. Section III investigates the symbol and bit error probabilities of the uncoded MFSK-based SFH/SS system over Nakagami-m fading channels. In Section IV we derive the associated PDFs of the OTT, RTT and MO-RTT erasure insertion schemes, and provide the necessary expressions for computing the codeword decoding error probability using "errors-and-erasures" decoding. Our numerical results are provided in Section V, and finally in Section VI we present our conclusions.

II. System Overview and Statistics of the Decision Variables

The system under consideration was described in [3], [9], [19], and the reader might like to consult these references for their description. In the system considered SFH/SS using MFSK modulation, noncoherent demodulation based on square-law detection, and an extended $\mathrm{RS}\,(N,K)$ code over GF(2^b) are employed. We assume that $M = N = 2^b \geq 4$, so that each b-bit RS code symbol describes an M-ary MFSK symbol. Furthermore, we assume that the RS code symbols are interleaved in the transmitter, in order to randomize the bursts of symbol errors. When using SFH spreading and MFSK modulation, the transmitted signal can be expressed as

$$s(t) = \sqrt{2P_sR_c} \sum_{n=-\infty}^{\infty} \sum_{i=-\infty}^{\infty} P_{T_c}(t - nT_c)P_{T_s}(t - iT_s) \cdot \cos[2\pi(f_n + f_i)t + \varphi_n + \varphi_i] \quad (1)$$

where P_s is the transmitted symbol's power without FEC, R_c is the coding rate, $P_{T_c}(t)$ and $P_{T_s}(t)$ are unit pulses of duration T_c and T_s, respectively, while T_c and T_s are the FH dwell interval and MFSK symbol duration, respectively. We assume that L MFSK/RS symbols are transmitted in each FH dwell interval, i.e., $T_c = LT_s$. Furthermore, in (1) f_n is the hopping frequency during the nth hopping interval, f_i is the ith tone frequency associated with the ith transmitted MFSK/RS data symbol. Finally, φ_n and φ_i are random phases during the nth FH interval and the ith symbol interval.

The FH patterns are modeled as sequences of independent random variables, each of which is uniformly distributed over the set of legitimate FH frequencies. For each FH tone, the channel is modeled as a frequency nonselective fading process obeying Nakagami-m distribution [20]–[23]. However, different FH tones encounter independent fading. Furthermore, the communication channel is assumed to be contaminated by both PBGI [19] and additive white Gaussian noise (AWGN). The PBGI occupies a fraction $\rho \leq 1$ of the band, and the power spectral density of this contaminating source is $N_I/2\rho$. The AWGN is included in the analysis for modeling the receiver's thermal noise, and it has a uniform spectral density of $N_0/2$. Thus, in the portion of the frequency band contaminated by PBGI, the total two-sided power spectral density of the noise is $N_n/2 = N_I/2\rho + N_0/2$. In the remainder of the band, the total noise power spectral density is $N_n/2 = N_0/2$. Based on the above assumptions, the received signal $r(t)$ at the input of the energy detector—given that the first of the M-ary MFSK signals is transmitted during the interval $(0, T_s]$—can be expressed as

$$r(t) = \alpha\sqrt{2P_sR_c}\cos[2\pi(f_n + f_1)t + \theta_1] + n(t) + n_J(t), \quad 0 < t \leq T_s \quad (2)$$

where we assumed that the phases due to channel delay, FH and data modulation are absorbed by θ_1, which is uniformly distributed over $(0, 2\pi]$, $n(t)$ represents the AWGN and $n_J(t)$ represents the PBGI. In (2) α is an amplitude fading parameter, which obeys Nakagami-m distribution having the PDF given by [20]

$$p_\alpha(r) = \frac{2r^{2m-1}}{\Gamma(m)}\left(\frac{m}{\Omega}\right)^m \exp\left(-\frac{mr^2}{\Omega}\right) \quad (3)$$

where $\Gamma(\cdot)$ is the gamma function [24], $\Omega = E[\alpha^2]$ and m is the Nakagami-m fading parameter, which characterizes the severity of the fading. For a more detailed discourse concerning the Nakagami-m distribution readers are referred to [20].

The demodulator consists of a bank of M parallel noncoherent square-law detectors [9], [19]. The detectors are followed by a decision device that employs a threshold test. The decision whether to erase or not is made independently for each MFSK/RS symbol. For those MFSK/RS symbols not erased, standard hard-decision demodulation is employed. The decision device is followed by an M-ary symbol deinterleaver and a decoder that employs "errors-and-erasures" RS decoding. Let $U_1, U_2, \ldots, U_M$ be the outputs of the M noncoherent square-law detectors, which are assumed to be independent random variables. Then, it can be shown that, if the first of the M-ary MFSK/RS symbols is transmitted, the corresponding energy detector's output U_1 obeys the noncentral chi-square distribution with two degrees of freedom, which is given by [24]

$$f_{U_1}(x|S^2) = \frac{1}{2\sigma^2}\exp\left(-\frac{S^2+x}{2\sigma^2}\right) I_0\left(\sqrt{x}\frac{S}{\sigma^2}\right), \quad x \geq 0 \quad (4)$$

where $I_0(\,)$ is the modified Bessel function of the first kind of order zero, S is the noncentral parameter, which can be derived as

$$\begin{aligned} S^2 &= \left(E\left[\int_0^{T_s} r(t)\cos[2\pi(f_n + f_1)t]dt\right]\right)^2 \\ &\quad + \left(E\left[\int_0^{T_s} r(t)\sin[2\pi(f_n + f_1)t]dt\right]\right)^2 \\ &= \frac{\alpha^2 P_s R_c T_s^2}{2} \end{aligned} \quad (5)$$

while $\sigma^2 = N_nT_s/4$, where $N_n = N_0 + N_I/\rho$ or $N_n = N_0$ depending on whether the FH tone is interfered by the PBGI. We assume that $\{U_i\}_{i=2}^M$ are independent identically distributed

(i.i.d.) variables. Then, the energy detector's output U_i for $i = 2,3,\ldots,M$ obeys the exponential distribution with its PDF given by

$$f_{U_i}(x) = \frac{1}{2\sigma^2}\exp\Big(-\frac{x}{2\sigma^2}\Big), \qquad x \geq 0 \tag{6}$$

where σ^2 is the same as that in (4).

After the normalization of $\{U_i\}$ by $2\sigma^2$, (4) and (6) can be written as

$$f_{U_1}(y|\gamma) = \exp(-[y+\gamma])I_0\left(\sqrt{4\gamma y}\right), \qquad y \geq 0 \tag{7}$$

$$f_{U_i}(y) = \exp(-y), \qquad i > 1, y \geq 0. \tag{8}$$

In (7)

$$\gamma = \frac{S^2}{2\sigma^2} = \gamma_c \cdot \frac{\alpha^2}{\Omega} \tag{9}$$

where $\gamma_c = R_c\Omega E_s/N_n = R_c\Omega bE_b/N_n$, $E_s = P_sT_s$ represents the transmitted energy per symbol without FEC, $b = \log_2 M$ represents the number of bits per MFSK/RS symbol, and finally, we have $N_n = N_0 + N_I/\rho$ with a probability of ρ, while $N_n = N_0$ holds with a probability of $(1-\rho)$.

Since α is a random variable obeying the Nakagami-m distribution of (3), with the aid of (3) it can be shown that the PDF of γ defined in Eq. (9) can be expressed as

$$f(\gamma) = \frac{\gamma^{m-1}}{\Gamma(m)}\left(\frac{m}{\gamma_c}\right)^m \exp\Big(-\frac{m\gamma}{\gamma_c}\Big), \qquad \gamma \geq 0. \tag{10}$$

After removing the conditioning on γ in $f_{U_1}(y|\gamma)$ of (7) by averaging it over the valid range of γ, which obeys the distribution of (10), the unconditional PDF of U_1 for transmission over the flat Nakagami-m fading channel can be expressed as[1]

$$f_{U_1}(y) = \left(\frac{m}{m+\gamma_c}\right)^m \exp\Big(-\frac{my}{m+\gamma_c}\Big) \cdot {}_1F_1\left(1-m,1;-\frac{\gamma_c y}{m+\gamma_c}\right), \qquad y \geq 0 \tag{11}$$

where ${}_1F_1(\ )$ is the confluent hyper-geometric function [25], which is defined as

$${}_1F_1(a,b;x) = \sum_{k=0}^{\infty}\frac{(a)_k x^k}{(b)_k k!}, \qquad b \neq 0,-1,-2,\ldots$$

where $(a)_k = a(a+1)(a+2)\cdots(a+k-1)$, $(a)_0 = 1$. Above we have given an overview of the SFH/SS systems considered, derived the statistics of the decision variables input to the MFSK demodulator [9] over flat Nakagami-m fading channels. With the aid of these PDFs the average error probabilities can now be derived for the SFH/SS systems considered without FEC.

[1]Since $(-n)_{n+1} = 0$, if n is a positive integer, then ${}_1F_1(-n,b,x)$ is the sum of only a limited number of terms, which can be expressed as

$${}_1F_1(-n,b,x) = \sum_{k=0}^{n}\frac{(-n)_k x^k}{(b)_k k!}.$$

Therefore, if m is a positive integer, (11) consists of the sum of a limited number of terms.

III. Error Performance Without FEC Coding

Let H_1 and H_0 represent the hypotheses of correct decisions and erroneous decisions concerning an M-ary symbol in the MFSK demodulator using hard-detection. Let $P_{N_n}(H_1)$ and $P_{N_n}(H_0)$ be the average correct and erroneous symbol probabilities, respectively, for a given value of N_n. Then, we have $P_{N_n}(H_1) = 1 - P_{N_n}(H_0)$. Furthermore, given the symbol error probability $P_{N_n}(H_0)$, the average BER can be expressed as [24]

$$P_{N_n}(b) = \frac{2^{b-1}}{M-1}P_{N_n}(H_0), \tag{12}$$

where b represents the number of bits per M-ary symbol, i.e., $b = \log_2 M$.

Remembering that the first M-ary symbol is transmitted, then, for a given value of N_n, the average erroneous symbol probability of $P_{N_n}(H_0)$ for M-ary orthogonal systems can be expressed as

$$\begin{aligned} P_{N_n}(H_0) &= 1 - P(U_2 < U_1, U_3 < U_1, \ldots, U_M < U_1), \\ &= 1 - \int_0^{\infty} f_{U_1}(y)\left[\int_0^y f_{U_2}(x)dx\right]^{M-1} dy \end{aligned} \tag{13}$$

where $f_{U_1}(y)$ and $f_{U_2}(x)$ are given by (11) and (8), respectively. Upon substituting them into the above equation and using the binomial expansion [24], it can be shown that

$$\begin{aligned} P_{N_n}(H_0) = 1 - \sum_{k=0}^{\infty}\sum_{n=0}^{M-1}(-1)^{k+n}\frac{(1-m)_k}{k!}\binom{M-1}{n} \\ \cdot \left(\frac{m}{m+\gamma_c}\right)^m\left(\frac{\gamma_c}{m+\gamma_c}\right)^{-1}\left(\frac{\gamma_c}{mn+n\gamma_c+m}\right)^{k+1}. \end{aligned} \tag{14}$$

For a Rayleigh fading channel associated with $m = 1$ in (3), we have $(1-m)_0 = 1$ and $(1-m)_k = 0$ for $k \neq 0$. In this case (14) can be simplified to

$$P_{N_n}(H_0) = \sum_{n=1}^{M-1}\frac{(-1)^{n+1}\binom{M-1}{n}}{1+n+n\gamma_c} \tag{15}$$

which represents the average erroneous symbol probability of M-ary orthogonal signaling given in [24, (14-4-47)] over flat Rayleigh fading channels.

Above we have derived the average erroneous symbol probability conditioned on a given value of N_n, as shown in (14). Since the fraction ρ of the band is jammed, the average erroneous symbol probability and BER considering both AWGN alone and AWGN plus PBGI can be written as

$$P(H_0) = (1-\rho)P_{N_0}(H_0) + \rho P_{N_0+N_I/\rho}(H_0) \tag{16}$$

$$P(b) = \frac{2^{b-1}}{M-1}P(H_0) \tag{17}$$

where $P_{N_0}(H_0)$ and $P_{N_0+N_I/\rho}(H_0)$ represent the average erroneous symbol probabilities, given that the corresponding FH tone is free from or is jammed by the PBGI. $P_{N_0}(H_0)$ and $P_{N_0+N_I/\rho}(H_0)$ can be computed according to (14) by employing $\gamma_c = R_c\Omega bE_b/N_0$ and $\gamma_c = R_c\Omega bE_b/(N_0+N_I/\rho)$, respectively.

IV. Performance Analysis Using "Errors-and-Erasures" Decoding

It is well known that in the context of RS coding, "errors-and-erasures" decoding is preferable to "error-correction-only" decoding, since more erasures than errors can be corrected. In order to take advantage of the powerful "errors-and-erasures" correction capability of the RS code concerned, it is essential to design efficient erasure insertion schemes. In this section, erasure insertion schemes using the OTT [12], RTT [5] as well as the joint MO-RTT [13] are investigated and the PDFs of the quantities involved in these erasure insertion schemes are derived. From these PDFs, we can gain an explicit insight into the properties of the related erasure insertion schemes. Furthermore, with the aid of these PDFs, the corresponding RS codeword decoding error probability using "errors-and-erasures" decoding can be evaluated using a numerical approach.

A. Statistics of the Erasure Insertion Related Variables

Let $\{U_1, U_2, \ldots, U_M\}$ represent the decision variables input to the MFSK demodulator of [9, Fig. 1]. We denote the maximum and the "second" maximum of $\{U_1, U_2, \ldots, U_M\}$ by

$$Y_1 = \max_1\{U_1, U_2, \ldots, U_M\} \tag{18}$$

$$Y_2 = \max_2\{U_1, U_2, \ldots, U_M\}. \tag{19}$$

In the context of the OTT, the decision variable subjected to an erasure insertion is Y_1, i.e., the actual demodulator output is observed. In order to analyze the properties of the OTT-based erasure insertion scheme and to evaluate its corresponding "errors-and-erasures" RS decoding performance, the PDFs $f_{Y_1}(y|H_1)$ and $f_{Y_1}(y|H_0)$, given that the associated demodulated symbol is correct (H_1) and incorrect (H_0), respectively, must be derived.

The ratio involved in Viterbi's RTT is defined as the ratio of the maximum to the "second" maximum [5], or equivalently, it can be defined as the ratio of the "second" maximum to the maximum, which can be expressed as

$$\lambda = \frac{Y_2}{Y_1}, \qquad 0 \le \lambda \le 1. \tag{20}$$

Similarly, in order to analyze the "errors-and-erasures" RS decoding performance in terms of the RTT, the PDFs of $f_\lambda(r|H_1)$ and $f_\lambda(r|H_0)$, given that the associated demodulated symbol is correct (H_1) and incorrect (H_0) will be derived.

Finally, in the context of the joint MO-RTT, the erasure insertion is based on the observation of both the maximum Y_1 of (18) and the ratio λ of (20). Hence, the joint two-dimensional (2-D) PDFs of $f_{Y_1,\lambda}(y, r|H_1)$ and $f_{Y_1,\lambda}(y, r|H_0)$ will be derived, in order to evaluate the "errors-and-erasures" RS decoding performance in terms of the joint MO-RTT erasure insertion scheme. Since $f_{Y_1}(y|H_\vartheta)$ and $f_\lambda(r|H_\vartheta)$ constitute the "marginal" PDFs of the joint PDFs of $f_{Y_1,\lambda}(y, r|H_\vartheta)$ associated with $\vartheta \in \{0, 1\}$, all the PDFs considered can be derived by first deriving the joint PDFs of $f_{Y_1,\lambda}(y, r|H_\vartheta)$ in terms of the MO-RTT.

As shown in the Appendix, the joint PDFs of Y_1 and $\lambda = Y_2/Y_1$ under the hypotheses H_1 of correction decision and H_0 of erroneous decision, respectively, can be expressed as

$$\begin{aligned} f_{Y_1,\lambda}(y, r|H_1) &= \frac{(M-1)y}{P_{N_n}(H_1)}\left(\frac{m}{m+\gamma_c}\right)^m \exp\left[-\left(\frac{m}{m+\gamma_c}+r\right)y\right] \\ &\quad \cdot [1-\exp(-yr)]^{M-2}{}_1F_1\left(1-m,\, 1;\, -\frac{\gamma_c y}{m+\gamma_c}\right), \\ &\quad 0 \le y < \infty,\ 0 \le r \le 1 \end{aligned} \tag{21}$$

$$\begin{aligned} f_{Y_1,\lambda}(y, r|H_0) &= \frac{(M-1)y}{P_{N_n}(H_0)}\left\{\left(\frac{m}{m+\gamma_c}\right)^m \exp\left(-\frac{(mr+m+\gamma_c)y}{m+\gamma_c}\right)\right. \\ &\quad \cdot [1-\exp(-yr)]^{M-2}{}_1F_1\left(1-m,\, 1;\, -\frac{\gamma_c yr}{m+\gamma_c}\right) \\ &\quad + (M-2)\exp[-(r+1)y][1-\exp(-yr)]^{M-3} \\ &\quad \left.\cdot [1-\Phi(yr)]\right\}, \qquad 0 \le y < \infty,\ 0 \le r \le 1 \end{aligned} \tag{22}$$

where $P_{N_n}(H_1)$ and $P_{N_n}(H_0)$ are the correct and erroneous symbol probabilities, respectively, for a given value of N_n, $P_{N_n}(H_1) = 1 - P_{N_n}(H_0)$, while $P_{N_n}(H_0)$ is given by (14). Furthermore, in (22) we have

$$\begin{aligned} \Phi(y) &= \int_y^\infty f_{U_1}(x)\,dx \\ &= \left(\frac{m}{m+\gamma_c}\right)^{m-1} \exp\left(-\frac{my}{m+\gamma_c}\right)\sum_{k=0}^{\infty}\sum_{n=0}^{k} \\ &\quad \cdot \frac{(1-m)_k}{k!n!}\left(-\frac{\gamma_c}{m}\right)^k \left(\frac{my}{m+\gamma_c}\right)^n. \end{aligned} \tag{23}$$

Upon integrating both sides of (21) and (22) in terms of the variable λ from zero to one, we obtain the PDFs of Y_1 under the hypotheses H_1 of correct decision and H_0 of erroneous decision, which can be expressed as

$$\begin{aligned} f_{Y_1}(y|H_1) &= \frac{1}{P_{N_n}(H_1)}\left(\frac{m}{m+\gamma_c}\right)^m \exp\left(-\frac{my}{m+\gamma_c}\right) \\ &\quad \cdot [1-\exp(-y)]^{M-1}{}_1F_1\left(1-m,\, 1;\, -\frac{\gamma_c y}{m+\gamma_c}\right), \\ &\quad 0 \le y < \infty \end{aligned} \tag{24}$$

$$f_{Y_1}(y|H_0) = \frac{M-1}{P_{N_n}(H_0)}\exp(-y)[1-\Phi(y)][1-\exp(-y)]^{M-2}, \quad 0 \le y < \infty. \tag{25}$$

Similarly, upon integrating both sides of (21) and (22) in terms of the variable y from zero to infinity, we arrive at the PDFs of $\lambda = Y_2/Y_1$ under the hypotheses H_1 of correct decision and H_0 of erroneous decision, which can be expressed as

$$\begin{aligned} f_\lambda(r|H_1) &= \frac{M-1}{P_{N_n}(H_1)}\left(\frac{m}{m+\gamma_c}\right)^m \sum_{k=0}^{\infty}\sum_{n=0}^{M-2}(-1)^{n+k} \\ &\quad \cdot \binom{M-2}{n}\frac{(k+1)(1-m)_k}{k!}\left(\frac{\gamma_c}{m+\gamma_c}\right)^k \\ &\quad \cdot \left(\frac{m+\gamma_c}{m+(m+\gamma_c)(n+1)r}\right)^{k+2}, \quad 0 \le r \le 1 \end{aligned} \tag{26}$$

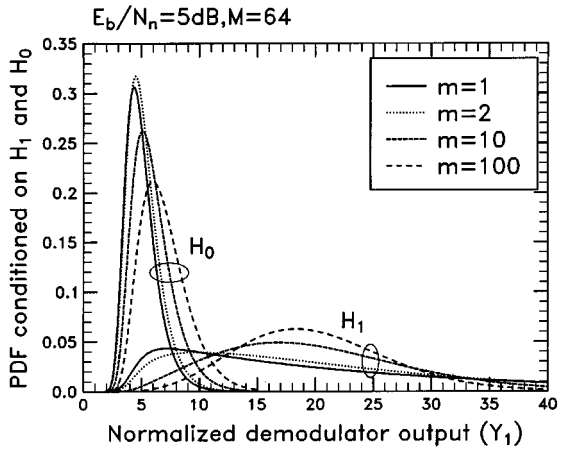

Fig. 1. The PDFs of $Y_1 = \max\{\cdot\}$ under the hypotheses of H_1 and H_0 using $M = 64$, average SINR per bit of $E_b/N_n = 5$ dB and Nakagami fading parameters of $m = 1, 2, 10, 1000$ over flat Nakagami-m fading channels.

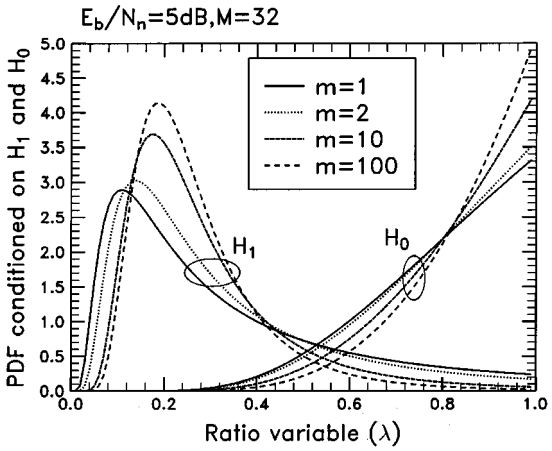

Fig. 2. The PDFs of $\lambda = Y_2/Y_1$ under the hypotheses of H_1 and H_0 using $M = 32$, an average SINR per bit of $E_b/N_n = 5$ dB and Nakagami fading parameters of $m = 1, 2, 10, 1000$.

$$f_\lambda(r|H_0) = \frac{M-1}{P_{N_n}(H_0)}\left\{\sum_{k=0}^{\infty}\frac{(1-m)_k}{k!}\left(\frac{m}{m+\gamma_c}\right)^{m-3}\right.$$
$$\cdot\left[\left(\frac{m}{\gamma_c r}\right)^2\left(\frac{m}{m+\gamma_c}\right)\sum_{n=0}^{M-2}(-1)^{n+k}\binom{M-2}{n}\right.$$
$$\cdot(k+1)\left(\frac{\gamma_c r}{(mn+n\gamma_c+m)r+m+\gamma_c}\right)^{k+2}$$
$$-(M-2)\sum_{j=0}^{k}\sum_{n=0}^{M-3}(-1)^{n+k}$$
$$\cdot(j+1)\left(\frac{\gamma_c}{m}\right)^k\binom{M-3}{n}r^{-2}$$
$$\left.\left.\times\left(\frac{mr}{(n+1)(m+\gamma_c)r+mr+m+\gamma_c}\right)^{j+2}\right]\right.$$
$$+(M-2)\sum_{n=0}^{M-3}(-1)^n\binom{M-3}{n}$$
$$\left.\cdot\left(\frac{1}{nr+r+1}\right)^2\right\}, \qquad 0\le r\le 1. \tag{27}$$

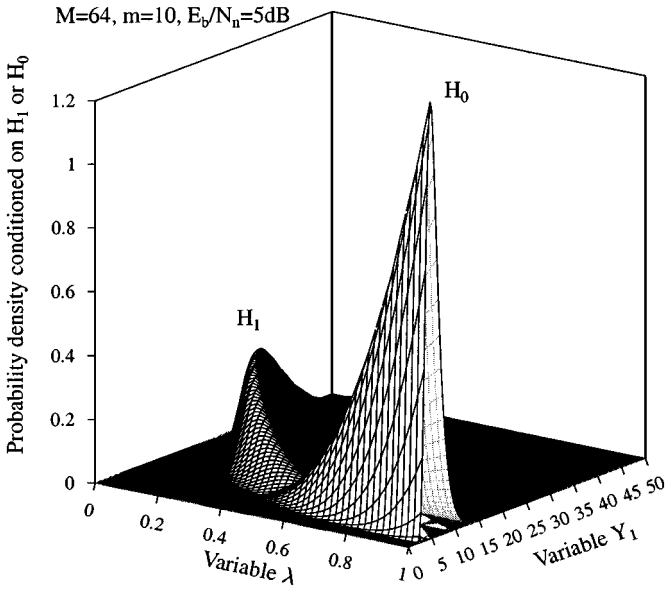

Fig. 3. The joint 2D PDFs of $f_{Y_1,\lambda}(y, r|H_1)$ and $f_{Y_1,\lambda}(y, r|H_0)$ using parameters of $M = 64, m = 10$ and an average SINR per bit of $E_b/N_n = 5$ dB over flat Nakagami-m fading channels.

The properties of the proposed OTT, Viterbi's RTT as well as MO-RTT can be studied with the aid of their corresponding PDFs $f_{Y_1}(y|H_1)$ and $f_{Y_1}(y|H_0)$ for the OTT shown in Fig. 1, $f_\lambda(r|H_1)$ and $f_\lambda(r|H_0)$ for the RTT shown in Fig. 2, while the joint 2D PDFs of $f_{Y_1,\lambda}(y, r|H_1)$ and $f_{Y_1,\lambda}(y, r|H_0)$ for the MO-RTT seen in Fig. 3 for a range of parameters, which are summarized in the figures. In the context of the OTT of Fig. 1, we observe that $f_{Y_1}(y|H_1)$ is mainly distributed over a normalized demodulator output range associated with relatively high values of Y_1, while $f_{Y_1}(y|H_0)$ is spread over a range having relatively low values of Y_1. Consequently, we can argue that the demodulated symbols having relatively low values of Y_1 are less reliable than those having relatively high values of Y_1. Let Y_T be a threshold associated with making an erasure decision based on the OTT. Then, if $Y_1 \le Y_T$, the associated demodulated symbol should be erased. Otherwise, if $Y_1 > Y_T$, the demodulator outputs a RS code symbol. In the context of the RTT of Fig. 2, we observe that $f_\lambda(r|H_1)$ is mainly spread over the range having relatively low values of λ, while $f_\lambda(r|H_0)$ is mainly distributed over the range having relatively high values of λ. Therefore, the demodulated symbols having a relatively low ratio of λ are more reliable, than those having relatively high values of λ. Consequently, a pre-set threshold λ_T can be invoked, in order to erase these low-reliability symbols associated with a ratio of $\lambda \ge \lambda_T$. Finally, in the context of the joint MO-RTT having PDFs of Fig. 3, we observe that for the given parameters the peak of the distribution $f_{Y_1,\lambda}(y, r|H_1)$ is located at a relatively high value of Y_1 or a relatively low value of λ, while the peak of the distribution $f_{Y_1,\lambda}(y, r|H_0)$ is located at a relatively low value of Y_1 and a relatively high value of λ. The above observations in turn imply that $f_{Y_1,\lambda}(y, r|H_1)$ is mainly spread over the range having relatively high values of Y_1 or relatively low values of λ, while $f_{Y_1,\lambda}(y, r|H_0)$ is mainly distributed over the range having relatively low values of Y_1 and relatively high values of λ. Therefore, if a demodulated symbol has a maximum output

value of Y_1 and a ratio of λ, that had fallen in the main range of $f_{Y_1,\lambda}(y,r|H_0)$, the symbol concerned must be a low-reliability symbol and must be replaced by an erasure. By contrast, if a demodulated symbol has values of Y_1 and λ that had fallen outside the main range of $f_{Y_1,\lambda}(y,r|H_0)$, then this symbol is likely to be correct and the corresponding RS code symbol can be forwarded to the RS decoder. Consequently, in order to erase the low-reliability RS coded symbols, we assume that Y_T and λ_T are two thresholds, which activate an erasure insertion, whenever $Y_1 \le Y_T$ and $\lambda \ge \lambda_T$.

B. Codeword Decoding Error Probability

In the previous subsection we have derived the required PDFs for the OTT, RTT, and MO-RTT erasure insertion schemes, in order to investigate the codeword decoding error probabilities associated with using "errors-and-erasures" RS decoding. Let us now compute the RS code symbol error probability and RS code symbol erasure probability, after the erasure insertion decision according to the OTT, RTT, or MO-RTT. Furthermore, we investigate the codeword decoding error probability using "errors-and-erasures" decoding by considering both that the receiver has perfect PBGI side-information or when the PBGI side-information is unavailable at the receiver. More explicitly, by side-information, we mean information concerning the presence or absence of interference on a given FH tone.

Let us assume that Y_T is a threshold associated with the OTT, λ_T is a threshold associated with the RTT, and furthermore, (Y_T, λ_T) are two thresholds associated with the MO-RTT, which activate an erasure insertion, whenever $Y_1 \le Y_T$ in terms of the OTT, $\lambda \ge \lambda_T$ in terms of the RTT, and $\{Y_1 \le Y_T\} \bigcap \{\lambda \ge \lambda_T\}$ in terms of the MO-RTT, respectively. Based on the properties of the OTT, RTT as well as MO-RTT, their corresponding symbol erasure probability, $P_e(\ )$, and random symbol error probability, $P_t(\ )$, after erasure insertion decision can be summarized as follows. Note that, since both the symbol erasure probability and random symbol error probability after erasure insertion decision are functions of the thresholds involved, the thresholds are explicitly presented in the following equations.

- **OTT**:

$$P_e(N_n, Y_T) = P_{N_n}(H_1) \int_0^{Y_T} f_{Y_1}(y|H_1)\, dy + P_{N_n}(H_0) \int_0^{Y_T} f_{Y_1}(y|H_0)\, dy, \tag{28}$$

$$P_t(N_n, Y_T) = P_{N_n}(H_0) \left[1 - \int_0^{Y_T} f_{Y_1}(y|H_0)\, dy \right] \tag{29}$$

  where the PDFs of $f_{Y_1}(y|H_1)$ and $f_{Y_1}(y|H_0)$ are given by (24) and (25), respectively.

- **RTT**:

$$P_e(N_n, \lambda_T) = P_{N_n}(H_1) \int_{\lambda_T}^{1} f_\lambda(r|H_1)\, dr + P_{N_n}(H_0) \int_{\lambda_T}^{1} f_\lambda(r|H_0)\, dr \tag{30}$$

$$P_t(N_n, \lambda_T) = P_{N_n}(H_0) \int_0^{\lambda_T} f_\lambda(r|H_0)\, dr \tag{31}$$

  where the PDFs of $f_\lambda(r|H_1)$ and $f_\lambda(r|H_0)$ are given by (26) and (27), respectively.

- **MO-RTT**:

$$P_e(N_n, Y_T, \lambda_T) = P_{N_n}(H_1) \int_0^{Y_T} \int_{\lambda_T}^{1} f_{Y_1,\lambda}(y, r|H_1)\, dr\, dy + P_{N_n}(H_0) \int_0^{Y_T} \int_{\lambda_T}^{1} f_{Y_1,\lambda}(y, r|H_0)\, dr\, dy \tag{32}$$

$$P_t(N_n, Y_T, \lambda_T) = P_{N_n}(H_0) \left[1 - \int_0^{Y_T} \int_{\lambda_T}^{1} f_{Y_1,\lambda}(y, r|H_0)\, dr\, dy \right] \tag{33}$$

  where $f_{Y_1,\lambda}(y, r|H_1)$ and $f_{Y_1,\lambda}(y, r|H_0)$ are the joint PDFs of Y_1 and λ of (21) and (22).

According to (28)–(33), we can see that the symbol erasure probability and random symbol error probability after erasure insertion decision are functions of the noise plus interference spectral densities and the thresholds. For a given transmitted power and for a given value of N_n, the thresholds can be optimized numerically, in order to achieve the minimum codeword decoding error probability. When the PBGI side-information associated with each RS code symbol is unavailable, the optimum thresholds can only be derived by minimizing the average codeword decoding error probability averaging over both the cases in the absence and in the presence of the PBGI. However, when perfect PBGI side-information is available at the receiver, then, it was shown in [9] that two different thresholds can be invoked for improving the performance. Specifically, one corresponding to the case of AWGN only, while the other one corresponding to the presence of AWGN plus PBGI. Consequently, the optimum thresholds associated with the OTT, RTT or MO-RTT can be derived by minimizing the average codeword decoding error probability by considering both the absence of PBGI and the presence of PBGI. This implies the optimization of thresholds Y_{T_1}, Y_{T_2} for the OTT, λ_{T_1}, λ_{T_2} for the RTT, or (Y_{T_1}, λ_{T_1}), (Y_{T_2}, λ_{T_2}) for the MO-RTT, respectively. Consequently, for the above thresholds invoked in the OTT, RTT or MO-RTT, the average symbol erasure probability and random symbol error probability after erasure insertion decision can be expressed as

- **OTT**:

$$P_e = (1-\rho) P_e(N_0, Y_{T_1}) + \rho P_e(N_0 + N_I/\rho, Y_{T_2}), \tag{34}$$

$$P_t = (1-\rho) P_t(N_0, Y_{T_1}) + \rho P_t(N_0 + N_I/\rho, Y_{T_2}) \tag{35}$$

- **RTT**:

$$P_e = (1-\rho) P_e(N_0, \lambda_{T_1}) + \rho P_e(N_0 + N_I/\rho, \lambda_{T_2}) \tag{36}$$

$$P_t = (1-\rho) P_t(N_0, \lambda_{T_1}) + \rho P_t(N_0 + N_I/\rho, \lambda_{T_2}) \tag{37}$$

- **MO-RTT**:

$$P_e = (1-\rho) P_e(N_0, Y_{T_1}, \lambda_{T_1}) + \rho P_e(N_0 + N_I/\rho, Y_{T_2}, \lambda_{T_2}) \tag{38}$$

$$P_t = (1-\rho)P_t(N_0, Y_{T_1}, \lambda_{T_1}) + \rho P_t(N_0 + N_I/\rho, Y_{T_2}, \lambda_{T_2}). \tag{39}$$

In (34)–(39), $\rho \leq 1$ is the fraction of the band that the PBGI contaminates, $P_e(N_0, \ldots)$, $P_t(N_0, \ldots)$ are the corresponding symbol erasure probability and random symbol error probability associated with absence of PBGI, while $P_e(N_0 + N_I/\rho, \ldots)$, $P_t(N_0 + N_I/\rho, \ldots)$ are the corresponding symbol erasure probability and random symbol error probability associated with presence of PBGI. Furthermore, we emphasize that if the knowledge of PBGI is unavailable at the receiver, in (34)–(39), the thresholds of Y_{T_1} and Y_{T_2}, λ_{T_1} and λ_{T_2} should be set to be equal, i.e., $Y_{T_1} = Y_{T_2}$, $\lambda_{T_1} = \lambda_{T_2}$, and then optimized, since the receiver is unaware, whether the received symbol is interfered.

Finally, based on the symbol erasure probability and random symbol error probability, if we assume that the symbol errors and symbol erasures within a RS codeword are independent due to using perfect symbol-based channel interleaving, then the codeword decoding error probability after "errors-and-erasures" RS(N, K) decoding can be expressed as [14]:

$$P_W = \sum_{i=0}^{N} \sum_{j=j_0(i)}^{N-i} \binom{N}{i} \binom{N-i}{j} P_t^i P_e^j (1 - P_t - P_e)^{N-i-j} \tag{40}$$

where $j_0(i) = \max\{0, N - K + 1 - 2i\}$, while P_e and P_t represent the symbol erasure probability and random symbol error probability before RS decoding, respectively, which are given by (34) and (35) for the OTT, (36) and (37) for the RTT, and (38) and (39) for the MO-RTT.

Above we have analyzed the codeword decoding error probability associated with the OTT, RTT and MO-RTT by using "errors-and-erasures" decoding. Let us now evaluate the system's performance for a range of parameters.

V. Performance Results

In this section the performance of the RS coded MFSK based SFH/SS system using "errors-and-erasures" decoding associated with the OTT, RTT or MO-RTT erasure insertion scheme is evaluated and compared for a range of parameters.

In Figs. 4 and 5 we investigated the influence of the PBGI duty factor, ρ, on the average BER performance of an uncoded MFSK based SFH/SS system over Nakagami-m fading channels for fading factors of $m = 1$, 2, 3, 4, 5, 10 and 100. The parameters of Fig. 4 were $M = 32$, signal to noise ratio (SNR) per bit of $E_b/N_0 = 10$ dB and SIR per bit of $E_b/N_I = 8$ dB. The parameters in Fig. 5 were the same as in Fig. 4, except for $E_b/N_I = 10$ dB. From the results of Figs. 4 and 5 we observe that for each curve associated with a fading factor of $m > 1$, there exists a PBGI duty factor, ρ, which results in the highest BER. By contrast, for the Rayleigh fading channel corresponding to $m = 1$, the maximum BER is observed, when $\rho = 1$, which implies that spreading the PBGI power over the whole band used results in the worst possible BER.

Figs. 6 and 7 show the codeword decoding error probability of (40) associated with (38) and (39) over the Rayleigh fading channel having $m = 1$ (Fig. 6) and Nakagami-m fading channel having $m = 2$ (Fig. 7) using the proposed

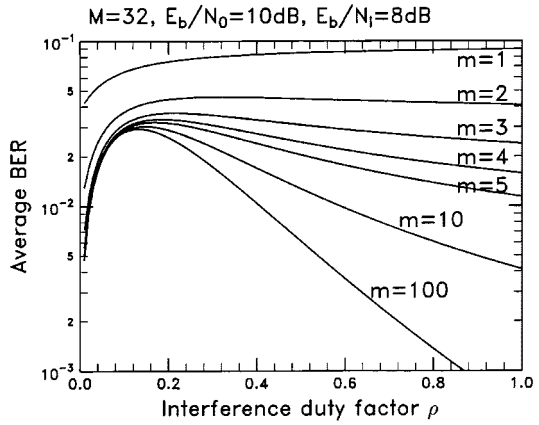

Fig. 4. Average BER versus PBGI duty factor, ρ, performance for the uncoded MSFK based SFH/SS system computed from (17) with the aid of (14) and (16).

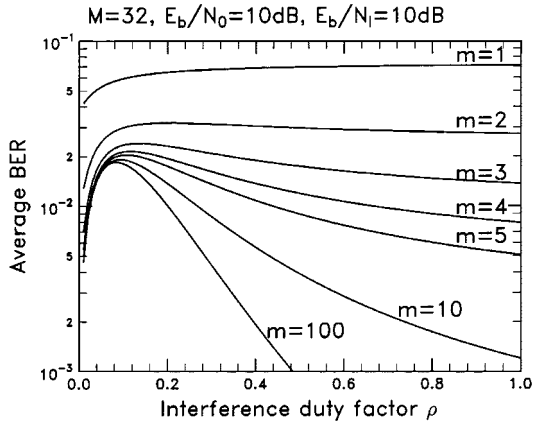

Fig. 5. Average BER versus PBGI duty factor, ρ, performance for the uncoded MSFK based SFH/SS system computed from (17) with the aid of (14) and (16).

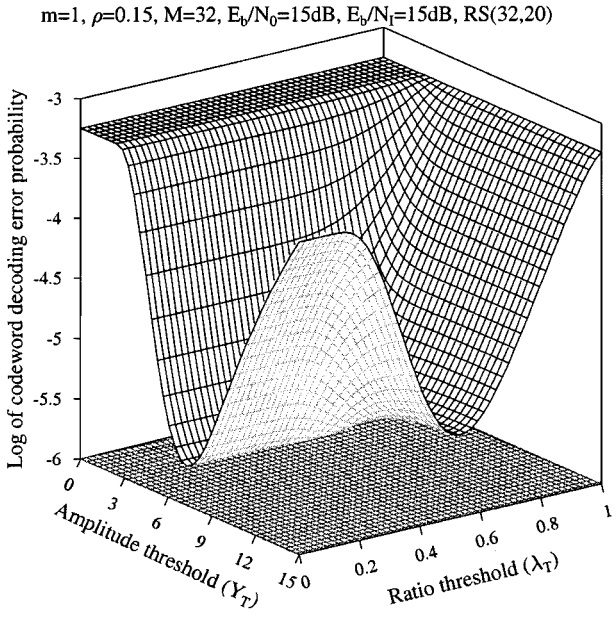

Fig. 6. Codeword decoding error probability versus the amplitude threshold, Y_T and the ratio threshold, λ_T for the RS(32, 20) FEC code using "errors-and-erasures" decoding based on the MO-RTT erasure insertion scheme over Rayleigh fading channels ($m = 1$). The results were evaluated from (40) with the aid of (38) and (39).

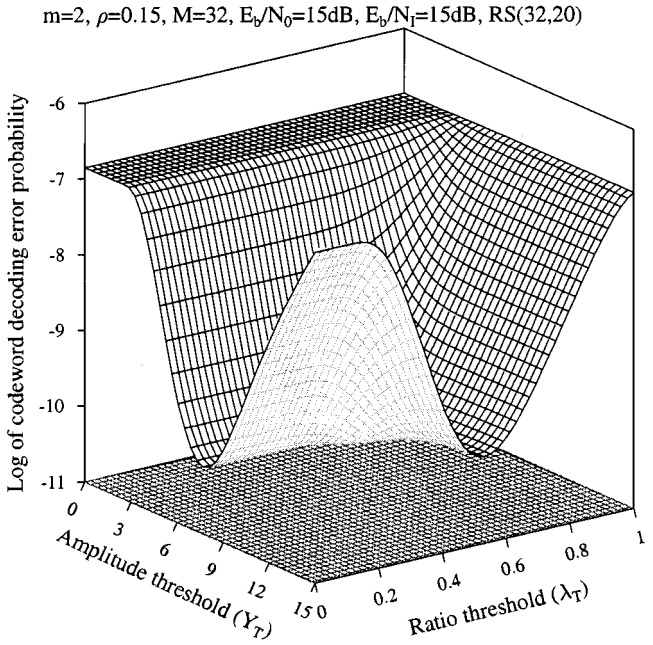

Fig. 7. Codeword decoding error probability versus the amplitude threshold, Y_T and the ratio threshold, λ_T for the RS(32, 20) FEC code using "errors-and-erasures" decoding based on the MO-RTT erasure insertion scheme over Nakagami-m fading channels for $m = 2$. The results were evaluated from (40) with the aid of (38) and (39).

joint MO-RTT. The RS(32, 20) code over the Galois Field GF(32) $= \mathrm{GF}(2^5)$ corresponding to 5-bit symbols was used and "errors-and-erasures" decoding based on the proposed MO-RTT insertion scheme was employed. From the results we observe that there exists an optimum threshold value of λ_T or Y_T, for which the "errors-and-erasures" decoding achieves the minimum codeword decoding error probability. This observation in turn implies that for given values of M, SNR per bit of E_b/N_0, SIR per bit of E_b/N_I as well as for a given RS code, there exist optimum thresholds of Y_T and λ_T, for which the "errors-and-erasures" decoding using the joint MO-RTT erasure insertion scheme achieves the minimum codeword decoding error probability. This minimum codeword decoding error probability is lower, than that associated with using the RTT alone or the OTT alone. Note that the point corresponding to $Y_T = 0$ and $\lambda_T = 1$ represents the codeword decoding error probability using "error-correction-only" decoding, i.e., no erasure insertion at all. Therefore, we can observe that for both cases considered, the "errors-and-erasures" decoding outperforms the "error-correction-only" decoding, if the appropriate thresholds are invoked. However, if the threshold Y_T is too high and simultaneously the threshold λ_T is too low, too many erasures will be activated, potentially erasing correct demodulated symbols. Consequently, the codeword decoding error probability using "errors-and-erasures" decoding might be higher, than that using "error-correction-only" decoding.

Since the optimum thresholds invoked in the OTT, RTT as well as MO-RTT can be derived numerically for a given range of parameters, in our further investigations we assumed that the optimum threshold was employed, whenever "errors-and-erasures" decoding was used. In Figs. 8 and 9 we evaluated the codeword decoding error probability of a RS(32, 20) coded

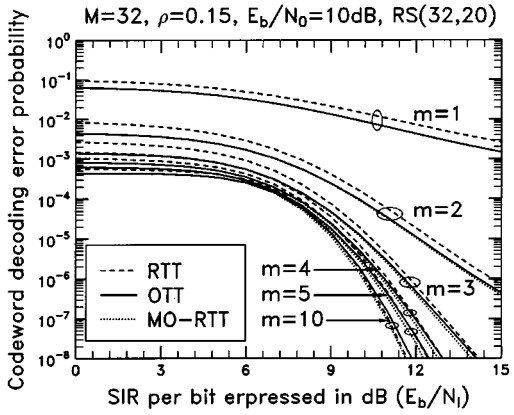

Fig. 8. Codeword decoding error probability versus SIR per bit for RS(32, 20) "erasures-and-erasures" decoding using the OTT, RTT and joint MO-RTT erasure insertion schemes. The results were computed from (40) with the aid of (34) and (35) for the OTT, using (36) and (37) for the RTT, and (38) and (39) for the MO-RTT, respectively.

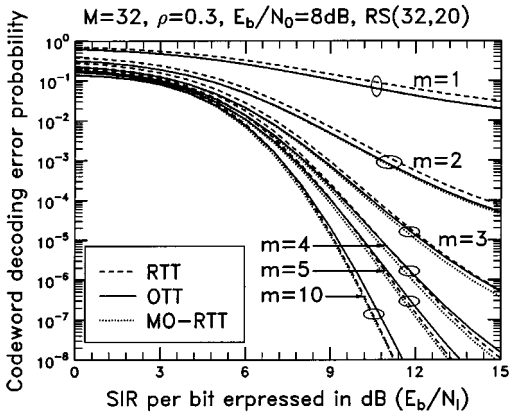

Fig. 9. Codeword decoding error probability versus SIR per bit for RS(32, 20) "erasures-and-erasures" decoding using the OTT, RTT and joint MO-RTT erasure insertion schemes. The results were computed from (40) with the aid of (34) and (35) for the OTT, using (36) and (37) for the RTT, and (38) and (39) for the MO-RTT, respectively.

MFSK based SFH/SS system employing the OTT, RTT and MO-RTT erasure insertion schemes over Nakagami-m fading channels having different fading parameters. The results were computed from (40) associated with (34) and (35) for the OTT, (36) and (37) for the RTT, and (38) and (39) for the MO-RTT erasure insertion schemes, respectively. The different parameters used when generating these two figures were $E_b/N_0 = 10$ dB, $\rho = 0.15$ associated with Fig. 8, while $E_b/N_0 = 8$ dB, $\rho = 0.3$ were employed in Fig. 9. From the results of Fig. 8 we observe that, when $m = 1, 2, 3, 4, 5$ or when the SIR expressed as E_b/N_I is sufficiently low, both the proposed OTT and MO-RTT erasure schemes outperform the RTT erasure insertion scheme. However, when the channel fading is not severe, characterized for example by the fading parameter of $m = 10$, we observe that the RTT outperforms the OTT, provided that the SIR is sufficiently high, for example, SIR > 9 dB. Similarly, from the results of Fig. 9 we observe that when $m = 1, 2, 3$ or when the SIR expressed as E_b/N_I is sufficiently low, both the OTT and MO-RTT erasure schemes outperform the RTT. However, when $m = 4, 5, 10$, and when the SIR is sufficiently high, we observe that the RTT outperforms the OTT. Furthermore,

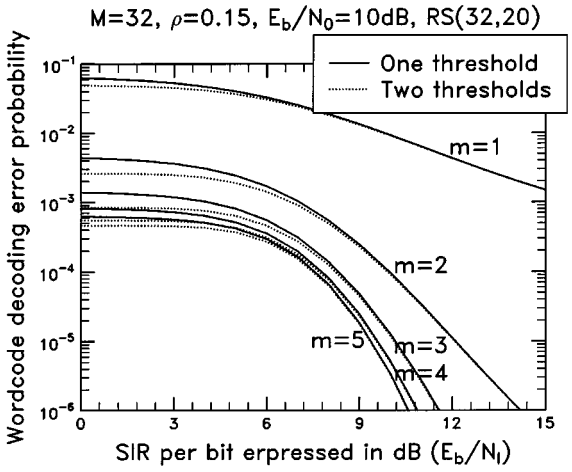

Fig. 10. Codeword decoding error probability versus SIR per bit for RS(32, 20) "erasures-and-erasures" decoding using the OTT erasure insertion scheme, with and without perfect PBGI side-information. The results were computed from (40) with the aid of (34) and (35).

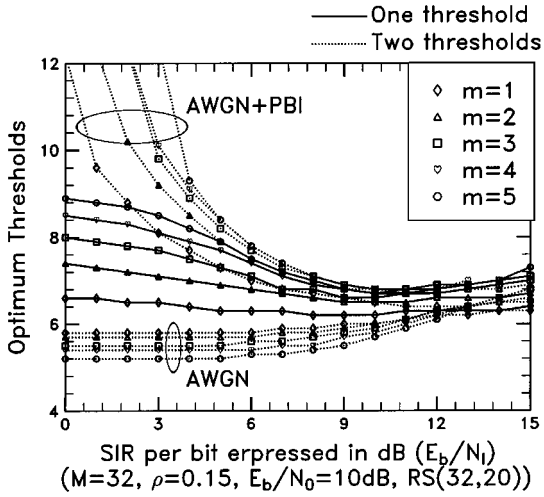

Fig. 11. Optimum thresholds invoked in the OTT for achieving the codeword decoding error probability versus SIR per bit performance shown in Fig. 10.

from the results of Figs. 8 and 9, as predicted, the MO-RTT erasure scheme outperforms both the RTT and the OTT erasure insertion schemes, provided that all the erasure insertion schemes are operated at the optimum decision thresholds. From the results we can also observe that, when the channel quality is relatively poor (characterized for example by $m = 1, 2$), the codeword decoding error probability of the OTT and MO-RTT becomes similar. By contrast, when the channel quality becomes better (for example in conjunction with $m = 5$, 10 in Fig. 9), the codeword decoding error probability of the RTT and MO-RTT becomes similar.

As we discussed previously in Section IV, when the receiver does not have any PBGI side-information, a single optimum threshold exists. However, if the PBGI side-information is available at the receiver, two optimum thresholds can be derived, in order to further enhance the RS "errors-and-erasures" decoding performance. Hence, as an example, in Fig. 10 we evaluated the codeword decoding error probability of a RS coded MFSK based SFH/SS system using the OTT erasure insertion scheme, when the PBGI side-information was unavailable at the receiver, or the receiver employed perfect PBGI side-information. Fig. 11 shows the optimum thresholds invoked in Fig. 10 for achieving the minimum possible codeword decoding error probability. From the results of Fig. 10 we observe that when the SIR per bit is lower than 9 dB, the codeword decoding error probability of the receiver benefiting from perfect PBGI side-information and associated with two optimum thresholds is lower than that without side-information and using one optimum threshold. However, when increasing the SIR per bit value, the codeword decoding error probability of the receiver using perfect PBGI side-information or that without PBGI side-information converges to the same value. The results of Fig. 11 show that when the SIR per bit is low, the optimum threshold corresponding to the symbols contaminated by PBGI is highly sensitive to the change of the SIR per bit value. By contrast, the optimum threshold corresponding to the uninterfered symbols, and the optimum threshold of the receiver having no PBGI side-information is relatively stable. However, when the SIR per bit value is sufficiently high, all the optimum thresholds converge to the relatively less sensitive values and vary over a limited range.

VI. Conclusions

In summary, we have proposed two novel erasure insertion schemes based on the OTT and MO-RTT, which have a similar complexity to the RTT, for RS coded SFH/SS communications using MFSK modulation. The exact PDFs of the decision variables in terms of the OTT, RTT and MO-RTT have been derived, when the channel is modeled as flat Nakagami-m fading in the presence of AWGN and PBGI, under the hypotheses that the M-ary demodulated symbol is correct (H_1) and incorrect (H_0). With the aid of these PDFs, we gained an insight into the basic characteristics of the OTT, Viterbi's RTT as well as the MO-RTT, and determined the optimum decision thresholds for these erasure insertion schemes, in order to achieve the minimum codeword decoding error probability using "errors-and-erasures" RS decoding for a range of parameters over Nakagami-m fading channels. The performance of RS coded SFH/SS systems using the OTT, RTT or MO-RTT based "errors-and-erasures" RS decoding has been investigated and compared over Nakagami-m fading channels, when noncoherent MFSK demodulation is considered. The numerical results suggest that when using "errors-and-erasures" decoding, RS codes of a given code rate can achieve a significantly higher coding gain, than without erasure information, provided that appropriate thresholds are invoked. Assuming that all schemes are operated at the optimum decision thresholds, we found that the OTT outperformed the RTT, when the channel fading was severe. However, the situation was reversed and the RTT outperformed the OTT, when the channel fading was moderate and the SIR was sufficiently high. Finally, the MO-RTT outperformed both the OTT and the RTT, regardless of the severity of the fading and the SIR experienced. Furthermore, the numerical results suggest that if explicit PBGI side-information is available at the receiver and if the interference power is high, two optimum thresholds—where one threshold is matched to the AWGN only and the other is matched to

the AWGN plus PBGI—can be employed, in order to further improve the performance of the investigated RS coded SFH/SS systems using "errors-and-erasures" decoding. The analysis in this paper can be extended to that of RS coded systems with or without spreading, where noncoherent M-ary orthogonal modulation, such as MFSK or Walsh function based orthogonal signaling is employed.

APPENDIX
DERIVATION OF THE JOINT PDFS $f_{Y_1,\lambda}(y, r|H_1)$ AND $f_{Y_1,\lambda}(y, r|H_0)$ INVOKED IN MO-RTT

In this appendix we derive the joint conditional PDFs $f_{Y_1,\lambda}(y, r|H_1)$ and $f_{Y_1,\lambda}(y, r|H_0)$ associated with the MO-RTT based erasure insertion scheme. These PDFs can be derived by first deriving the joint conditional PDFs of the maximum, Y_1, defined in (18), and that of the "second" maximum, Y_2, defined in (19). Once these PDFs are obtained, the joint conditional PDFs $f_{Y_1,\lambda}(y, r|H_1)$ and $f_{Y_1,\lambda}(y, r|H_0)$ can be readily derived by invoking the transformation techniques of [26]. Remembering the assumption that the first M-ary symbol is transmitted, then U_1 represents the decision variable corresponding to the transmitted symbol, which obeys the PDF of (11), while $\{U_2, U_3, \ldots, U_M\}$ are constituted by noise, which obey the i.i.d. having the PDF of (8). Consequently, for the hypothesis H_1, the joint PDF of Y_1 in (18) and Y_2 of (19) can be expressed as

$$\begin{aligned}
&f_{Y_1,Y_2}(y_1, y_2|H_1)\\
&\quad=\frac{\partial^2}{\partial y_1\,\partial y_2}P(Y_1\le y_1, Y_2\le y_2|H_1)\\
&\quad=\frac{1}{P_{N_n}(H_1)}\frac{\partial^2}{\partial y_1\,\partial y_2}P(Y_1\le y_1, Y_2\le y_2, H_1)\\
&\quad=\frac{1}{P_{N_n}(H_1)}\frac{\partial^2}{\partial y_1\,\partial y_2}\\
&\qquad\cdot P(Y_1=U_1\le y_1, Y_2=\max\{U_2,U_3,\ldots,U_M\}\le y_2)\\
&\quad=\frac{M-1}{P_{N_n}(H_1)}\frac{\partial^2}{\partial y_1\,\partial y_2}\\
&\qquad\cdot P\big(U_m\le U_1\le y_1, U_m\le y_2, \{U_j\le U_m\}_{j=2,\,j\ne m}^{M}\big)\\
&\quad=\frac{M-1}{P_{N_n}(H_1)}\frac{\partial^2}{\partial y_1\,\partial y_2}\left\{\int_0^{y_2}f_{U_m}(x)\,dx\right.\\
&\qquad\left.\cdot\left[\int_x^{y_1}f_{U_1}(y)\,dy\right]\left[\int_0^{x}f_{U_j}(y)\,dy\right]^{M-2}\right\}. \qquad (41)
\end{aligned}$$

In (41) $P_{N_n}(H_1)$ represents the probability that the demodulator output is correct at a given value of N_n. Upon executing the partial differential operations in (41) associated with y_1 and y_2, the joint PDF of Y_1 and Y_2—which are expressed as (18) and (19), respectively— under the hypothesis H_1 can be expressed as

$$\begin{aligned}
&f_{Y_1,Y_2}(y_1, y_2|H_1)\\
&\quad=\frac{M-1}{P_{N_n}(H_1)}f_{U_1}(y_1)f_{U_m}(y_2)\left[\int_0^{y_2}f_{U_j}(y)\,dy\right]^{M-2},\\
&\qquad y_1\ge y_2\ge 0. \qquad (42)
\end{aligned}$$

Let $Y_1=Y$, $Y_2=Y\lambda$. Then, it can be shown that the absolute value of the Jacobian of the transformation [26] is given by $|J|=Y$. Consequently, upon using this transformation in (42), the joint PDFs of Y_1 and λ under the hypothesis H_1 of correction decision can be expressed as

$$\begin{aligned}
&f_{Y_1,\lambda}(y, r|H_1)\\
&\quad=\frac{(M-1)y}{P_{N_n}(H_1)}f_{U_1}(y)f_{U_m}(yr)\left[\int_0^{yr}f_{U_j}(x)\,dx\right]^{M-2},\\
&\qquad 0\le y<\infty,\ 0\le r\le 1 \qquad (43)
\end{aligned}$$

where $f_{U_1}(y)$ is the PDF of the decision variable matched to the transmitted symbol, while, $f_{U_m}(x)$ and $f_{U_j}(x)$ represent the PDFs of the decision variables mismatched to the transmitted symbol. Upon using these PDFs in the above equation, the joint PDFs of Y_1 and λ under the hypothesis of H_1 can be expressed as seen in (21).

A. PDF Under the Hypothesis H_0

For the hypothesis H_0, the joint PDF of Y_1 in (18) and Y_2 of (19) can be expressed as

$$\begin{aligned}
&f_{Y_1,Y_2}(y_1, y_2|H_0)\\
&\quad=\frac{\partial^2}{\partial y_1\,\partial y_2}P(Y_1\le y_1, Y_2\le y_2|H_0)\\
&\quad=\frac{1}{P_{N_n}(H_0)}\frac{\partial^2}{\partial y_1\,\partial y_2}P(Y_1\le y_1, Y_2\le y_2, H_0)\\
&\quad=\frac{M-1}{P_{N_n}(H_0)}\frac{\partial^2}{\partial y_1\,\partial y_2}\\
&\qquad\cdot\{P\big(U_m=Y_1\le y_1, U_1=Y_2\le y_2, \{U_j\le U_1\}_{j=2,j\ne m}^{M}\big)\\
&\qquad+(M-2)P(U_m=Y_1\le y_1, U_j=Y_2\le y_2,\\
&\qquad\{U_k\le U_j\}_{k=1,\,k\ne m,\,j}^{M}\big)\}. \qquad (44)
\end{aligned}$$

In (44) $P_{N_n}(H_0)$ represents the probability that for given value of N_n, the demodulator output is in error. In deriving the third step from the second step, we assumed that the maximum of the decision variables $\{U_1, U_2, \ldots, U_M\}$ was $U_m\ne U_1$, since the demodulated M-ary symbol is in error. Furthermore, when proceeding from the second step to the third step, the "second" maximum has been divided into two cases. Specifically, the first case is when U_1 is the "second" maximum, which is described by the first term of the third step, while the second case is when U_1 is not the "second" maximum, i.e., the "second" maximum is also associated with a decision variable mismatched to the transmitted symbol. This case is described by the second term of the third step. Upon using the PDFs of the decision variables, $\{U_1, U_2, \ldots, U_M\}$, (44) can be further written as

$$\begin{aligned}
&f_{Y_1,Y_2}(y_1, y_2|H_0)\\
&\quad=\frac{M-1}{P_{N_n}(H_0)}\frac{\partial^2}{\partial y_1\,\partial y_2}\left\{\int_0^{y_2}f_{U_1}(x)\,dx\left[\int_x^{y_1}f_{U_m}(y)\,dy\right]\right.\\
&\qquad\cdot\left[\int_0^{x}f_{U_j}(y)\,dy\right]^{M-2}+(M-2)\int_0^{y_2}f_{U_j}(x)\,dx\\
&\qquad\cdot\left[\int_x^{y_1}f_{U_m}(y)\,dy\right]\left[\int_0^{x}f_{U_1}(y)\,dy\right]\\
&\qquad\left.\cdot\left[\int_0^{x}f_{U_k}(y)\,dy\right]^{M-3}\right\}. \qquad (45)
\end{aligned}$$

Upon executing the partial differential operations in (45) associated with y_1 and y_2, the joint PDF of Y_1 and Y_2 under the hypothesis H_0 can be formulated as

$$\begin{aligned} f_{Y_1,Y_2}(y_1, y_2|H_0) &= \frac{M-1}{P_{N_n}(H_0)}\left\{ f_{U_m}(y_1) f_{U_1}(y_2)\left[\int_0^{y_2} f_{U_j}(y)\,dy\right]^{M-2} \right. \\ &\quad + (M-2) f_{U_m}(y_1) f_{U_j}(y_2)\left[\int_0^{y_2} f_{U_1}(y)\,dy\right] \\ &\quad \left. \cdot \left[\int_0^{y_2} f_{U_k}(y)\,dy\right]^{M-3}\right\}, \qquad y_1 \geq y_2 \geq 0. \end{aligned} \tag{46}$$

Upon using the transformation techniques of [26] in (46), as in (42), the joint PDFs of Y_1 and λ under the hypothesis H_0 of erroneous decision can be expressed as

$$\begin{aligned} f_{Y_1,\lambda}(y, r|H_0) &= \frac{(M-1)y}{P_{N_n}(H_0)}\left\{ f_{U_m}(y) f_{U_1}(yr)\left[\int_0^{yr} f_{U_j}(x)\,dx\right]^{M-2} \right. \\ &\quad + (M-2) f_{U_m}(y) f_{U_j}(yr)\left[\int_0^{yr} f_{U_1}(x)\,dx\right] \\ &\quad \left. \cdot \left[\int_0^{yr} f_{U_k}(x)\,dx\right]^{M-3}\right\}, \quad 0 \leq y < \infty,\ 0 \leq r \leq 1 \end{aligned} \tag{47}$$

where $f_{U_1}(x)$ represents the PDF of (11), while, $f_{U_m}(x)$, $f_{U_j}(x)$ and $f_{U_k}(x)$ represent the PDFs of (8). Upon substituting these PDFs in the above equation, the joint PDFs of Y_1 and λ under the hypothesis of H_0 can be expressed as in (22).

ACKNOWLEDGMENT

The authors would like to acknowledge the contributions of their colleagues from Siemens AG, France Télécom - CNET, Centre Suisse d'Electronique et de Microtechnique S.A., King's College London, Motorola Ltd., Panasonic European Laboratories GmbH, Robert Bosch GmbH, Telefonica Investigacion Y Desarrollo S.A. Unipersonal, Toshiba Research Europe Ltd., TTI Norte S.L., University of Bristol, and University of Southampton. They would also like to thank the anonymous reviewers for their constructive suggestions and comments. They are particularly grateful to the reviewer, who pointed out an error in deriving (27) in the original manuscript and provided the correct derivation.

REFERENCES

[1] W. E. Stark, "Coding for frequency-hopping spread-spectrum communication with partial-band interference—Part I: Capacity and cutoff rate," *IEEE Trans. Commun.*, vol. 33, pp. 1036–1044, Oct. 1985.

[2] ——, "Coding for frequency-hopping spread-spectrum communication with partial-band interference—Part II: Coded performance," *IEEE Trans. Commun.*, vol. 33, pp. 1045–1057, Oct. 1985.

[3] M. B. Pursley and W. E. Stark, "Performance of Reed–Solomon coded frequency-hop spread-spectrum communications in partial-band interference," *IEEE Trans. Commun.*, vol. 33, pp. 767–774, Aug. 1985.

[4] S. W. Kim and W. Stark, "Optimum rate Reed–Solomon codes for frequency-hopped spread-spectrum multiple-access communication systems," *IEEE Trans. Commun.*, vol. 37, pp. 138–144, Feb. 1989.

[5] A. J. Viterbi, "A robust ratio-threshold technique to mitigate tone and partial band jamming in coded MFSK systems," in *Proc. IEEE Military Commun. Conf. Rec.*: IEEE, Oct. 1982, pp. 22.4.1–22.4.5.

[6] L.-F. Chang and R. J. McEliece, "A study of Viterbi's ratio threshold AJ technique," in *Proc. IEEE Military Commun. Conf. Rec.*: IEEE, Oct. 1984, pp. 182–186.

[7] C. M. Keller and M. B. Pursley, "Diversity combining for channels with fading and partial-band interference," *IEEE J. Select. Areas Commun.*, vol. SAC-5, pp. 248–259, Feb. 1987.

[8] Q. Wang and Y. Chao, "Frequency-hopped multiple access communications with coding and side information," *IEEE J. Select. Areas Commun.*, vol. 10, pp. 317–327, Feb. 1992.

[9] Y. T. Su and L. der Jeng, "Antijam capability analysis of RS-coded slow frequency-hopped system," *IEEE Trans. Commun.*, vol. 48, pp. 270–281, Feb. 2000.

[10] L.-L. Yang and L. Hanzo, "Errors-and-erasures decoding of Reed–Solomon codes over frequency-selective Rayleigh fading channel using M-ary orthogonal signaling," in *Proc. IEEE VTC'2000*, Tokyo, Japan, May 2000, pp. 854–858.

[11] L.-L. Yang, K. Yen, M. Dillinger, and L. Hanzo, "Performance of RS coded DS-CDMA using noncoherent M-ary orthogonal modulation over multipath fading channels," in *Proc. PIMRC'2000*, London, UK, Sept. 2000, pp. 584–588.

[12] L.-L. Yang and L. Hanzo, "Performance analysis of coded M-ary orthogonal signaling using errors-and-erasures decoding over frequency-selective fading channels," *IEEE J. Select. Areas Commun.*, vol. 19, no. 2, pp. 211–221, Feb. 2001.

[13] L.-L. Yang, K. Yen, and L. Hanzo, "A Reed–Solomon coded DS-CDMA system using noncoherent M-ary orthogonal modulation over multipath fading channels," *IEEE J. Select. Areas Commun.*, vol. 18, no. 11, pp. 2240–2251, Nov. 2000.

[14] C. W. Baum and M. B. Pursley, "Bayesian methods for erasure insertion in frequency-hop communication system with partial-band interference," *IEEE Trans. Commun.*, vol. 40, pp. 1231–1238, July 1992.

[15] ——, "A decision-theoretic approach to the generation of side information in frequency-hop multiple-access communications," *IEEE Trans. Commun.*, vol. 43, pp. 1768–1777, Feb./Mar./Apr. 1995.

[16] ——, "Bayesian generation of dependent erasures for frequency-hop communications and fading channels," *IEEE Trans. Commun.*, vol. 44, pp. 1720–1729, Dec. 1996.

[17] ——, "Erasure insertion in frequency-hop communications with fading and partial-band interference," *IEEE Trans. Veh. Technol.*, vol. 46, pp. 949–956, Nov. 1997.

[18] S. D. Fina and G. E. Corraza, "Bayesian approach for erasure insertion in frequency-hop multiple-access communications with selective fading," *IEEE Trans. Commun.*, vol. 48, pp. 282–289, Feb. 2000.

[19] R. E. Ziemer and R. L. Peterson, *Digital Communications and Spread Spectrum Systems*. New York: Macmillan, 1985.

[20] M. K. Simon and M.-S. Alouini, "A unified approach to the performance analysis of digital communication over generalized fading channels," *Proc. IEEE*, vol. 86, pp. 1860–1877, Sept. 1998.

[21] L.-L. Yang and L. Hanzo, "Blind soft-detection assisted frequency-hopping multicarrier DS-CDMA systems," in *Proc. IEEE GLOBECOM'99*, Rio de Janeiro, Brazil, Dec. 5–9, 1999, pp. 842–846.

[22] ——, "Slow frequency-hopping multicarrier DS-CDMA for transmission over Nakagami multipath fading channels," *IEEE J. Select. Areas Commun.*, vol. 19, no. 7, pp. 1211–1221, July 2001.

[23] ——, "Blind joint soft-detection assisted slow frequency-hopping multicarrier DS-CDMA," *IEEE Trans. Commun.*, vol. 48, pp. 1520–1529, Sept. 2000.

[24] J. G. Proakis, *Digital Communications*, 3rd ed: McGraw Hill, 1995.

[25] M. Abramowitz and I. A. Stegun, Eds., *Handbook of Mathematical Functions—With Formulas, Graphs, and Mathematical Tables*. New York: Dover, 1972.

[26] H. J. Larson and B. O. Shubert, *Probabilitic Models in Engineering Sciences, Volume I: Random Variables and Stochastic Processes*. New York: Wiley, 1979.

Lie-Liang Yang (M'98) received his B.Eng. degree in communication engineering from Shanghai TieDao University, Shanghai, China, in 1988, and the M.S., Ph.D. degrees in communications and electronics from Northern Jiaotong University, Beijing, China, in 1991 and 1997, respectively.

From 1991 to 1993, he was a Lecturer with the Department of Electrical Engineering, East-China Jiaotong University, China. From 1993 to 1997, he was with the Modern Communications Research Institute, Northern Jiaotong University, China. From June 1997 to Dec. 1997, he was a visiting scientist of the Institute of Radio Engineering and Electronics, Academy of Sciences of the Czech Republic. Since Dec. 1997, he has been with the Communication Group, Department of Electronics and Computer Science, University of Southampton, U.K., and has been involved in researching various error-correction coding, modulation, and detection techniques, as well as wideband, broadband and ultra wideband CDMA systems for the advanced wireless mobile communication systems. He has published over 60 papers in journals and conference proceedings.

Dr. Yang was awarded the Royal Society Sino-British Fellowship in 1997.

Lajos Hanzo (M'91–SM'92) graduated in electronics in 1976 and received the Ph.D. degree in 1983.

During his 25-year career in telecommunications, he has held various research and academic posts in Hungary, Germany, and the U.K. Since 1986, he has been with the Department of Electronics and Computer Science, University of Southampton, U.K, and has been a consultant to Multiple Access Communications Ltd., U.K. Currently, he holds the Chair of Telecommunications at the University of Southampton. He coauthored eight books on mobile radio communications, published in excess of 400 research papers, organized and chaired conference sessions, presented overview lectures and was awarded a number of distinctions. His current research interests are in the field of wireless multimedia communications. His work is sponsored both by industry, the Engineering and Physical Sciences Research Council (EPSRC) U.K, the European IST Programme and the Mobile Virtual Centre of Excellence (VCE), U,K.